Electrochemical and
Solid-State Letters

Remote Plasma ALD of Platinum and Platinum Oxide Films

To cite this article: H. C. M. Knoops *et al* 2009 *Electrochem. Solid-State Lett.* **12** G34

Electrochemical and Solid-State Letters, **12** (7) G34-G36 (2009)
1099-0062/2009/12(7)/G34/3/$25.00 © The Electrochemical Society

Remote Plasma ALD of Platinum and Platinum Oxide Films

H. C. M. Knoops,[a,b,*,z] A. J. M. Mackus,[b] M. E. Donders,[a,b] M. C. M. van de Sanden,[b] P. H. L. Notten,[b,c,] and W. M. M. Kessels[b,**,z]**

[a]*Materials Innovation Institute M2i, 2600 GA Delft, The Netherlands*
[b]*Eindhoven University of Technology, 5600 MB Eindhoven, The Netherlands*
[c]*Philips Research, 5656 AE Eindhoven, The Netherlands*

Platinum and platinum oxide films were deposited by remote plasma atomic layer deposition (ALD) from the combination of (methylcyclopentadienyl)trimethylplatinum ($MeCpPtMe_3$) precursor and O_2 plasma. A short O_2 plasma exposure (0.5 s) resulted in low resistivity (15 $\mu\Omega$ cm), high density (21 g/cm^3), cubic Pt films, whereas a longer O_2 plasma exposure (5 s) resulted in semiconductive PtO_2 films. In situ spectroscopic ellipsometry studies revealed no significant nucleation delay, different from the thermal ALD process with O_2 gas which was used as a benchmark. A broad temperature window (100–300°C) for remote plasma ALD of Pt and PtO_2 was demonstrated.
 [DOI: 10.1149/1.3125876]

Manuscript submitted February 20, 2009; revised manuscript received April 7, 2009. Published April 27, 2009.

When deposited with the precise thickness control and high conformality of atomic layer deposition (ALD), platinum films have a large variety of potential applications in microelectronics and energy technologies due to their chemical stability, catalytic activity, and excellent electronic properties.[1-7] While being less investigated, platinum oxide is of interest because of its optical properties and because PtO_x can be (locally) reduced to Pt.[8-10] In the research efforts toward the applications of these films deposited by ALD, nucleation properties, material quality, and process temperature window are of key importance.

Few Pt ALD processes have been reported, of which the thermal ALD process using (methylcyclopentadienyl)trimethylplatinum ($MeCpPtMe_3$) and O_2 gas described by Aaltonen et al.[1] has become the most adopted.[2,3] This process relies on the dissociative chemisorption of O_2 on the Pt surface for oxidative decomposition of the precursor ligands.[11,12] For PtO_x only one ALD process has been reported, to the best of our knowledge.[13] PtO_x films were obtained from the combination of $Pt(acac)_2$ (acac = acetylacetonate) and O_3 in the small temperature window of 120–130°C.[13]

In this article, ALD processes are reported for Pt and PtO_2 from the combination of $MeCpPtMe_3$ precursor and O_2 plasma exposure. In the O_2 plasma, O radicals are created, providing atomic O to the surface directly from the gas phase, enhancing oxygen chemisorption and oxidation.[14] The growth and nucleation properties, material properties, and substrate-temperature dependence of the Pt and PtO_2 process are investigated for remote plasma ALD and benchmarked against the thermal ALD of Pt.

Experimental

The Pt and PtO_2 films were deposited in the open-load ALD-I setup described extensively in Ref. 15. In short, a deposition chamber was connected to an inductively coupled plasma source and a pump unit through gate valves. The pump unit consisted of a turbo molecular pump and a rotary pump reaching a base pressure of $<10^{-5}$ mbar by overnight pumping. $MeCpPtMe_3$ precursor (98%, Sigma-Aldrich), heated to 70°C, was vapor drawn into the chamber. The substrates were heated to 100–300°C (precursor decomposition starts above 310°C),[3] while the reactor walls were kept at a temperature of 75°C.

For the processes investigated the first half-cycle consisted of $MeCpPtMe_3$ precursor dosing with the bottom valve closed (no pumping) to maximize precursor usage. After the precursor exposure the reaction products were pumped out by opening the bottom valve to the turbo pump. For thermal ALD the second half-cycle consisted of a 5 s O_2 exposure at 0.03 mbar. For the remote plasma process the O_2 gas flowed through the plasma source (0.01 mbar pressure) while a 100 W plasma power was applied. A 0.5 s O_2 plasma exposure was used for Pt deposition, while a 5 s plasma exposure resulted in the deposition of PtO_2 films. Si(100) with native oxide or with 400 nm thermally grown SiO_2 was used as the substrate.

In situ spectroscopic ellipsometry (SE) with a J. A. Woollam, Inc. M2000U (0.75–5.0 eV) ellipsometer was employed to determine the thickness and the dielectric function of the films during the ALD process. After deposition the optical range was extended to 6.5 eV using ex situ variable-angle measurements with a J. A. Woollam, Inc. M2000D.[15] Electrical resistivity was measured by a four-point probe (FPP), whereas the atomic composition and mass density of the films were determined from Rutherford backscattering spectrometry (RBS) using 2 MeV $^4He^+$ ions. The microstructure of the films was studied using X-ray diffraction (XRD) with a Philips X'Pert MPD diffractometer equipped with a Cu Kα source (1.54 Å radiation). Additionally, the thickness and mass density were determined by X-ray reflectometry (XRR) measurements on a Bruker D8 Advance X-ray diffractometer. The surface roughness of the films was determined by atomic force microscopy (AFM) using an NT-MDT Solver P47 SPM.

Results and Discussion

ALD growth and nucleation delay.— Pt films were deposited by remote plasma and thermal ALD, and PtO_2 was deposited by remote plasma ALD at a substrate temperature of 300°C. A summary of the conditions and material properties is given in Table I. For the thermal process a $MeCpPtMe_3$ dosing time of 1 s is necessary to reach saturation of the growth per cycle, while the remote plasma process requires 3 s. The length of the plasma exposure time determines whether Pt or PtO_2 is deposited. A short O_2 plasma exposure of 0.5 s results in Pt, while a long O_2 plasma exposure of 5 s results in PtO_2. When using O_2 gas, Pt is obtained up to long O_2 exposure times in line with the results reported by Aaltonen et al.[1]

When measuring the thickness as a function of the number of cycles by in situ SE for the three processes (Fig. 1), no growth was observed for thermal ALD on c-Si substrates with 400 nm SiO_2 or native oxide for the conditions employed. Pt growth on these substrates could only be achieved by using a higher O_2 pressure (>0.8 mbar) as also typically used in the literature.[1,3] On the contrary, remote plasma ALD of Pt (0.5 s O_2 plasma) leads to immediate growth without a substantial nucleation delay. From the ellipsometry measurements, which have a reduced accuracy in the first 1–2 nm, it is concluded that growth per cycle is constant after the first 50 cycles. On the Pt film deposited by remote plasma ALD, the thermal ALD process continues without nucleation delay, demonstrating the possibility to deposit a Pt seed layer by remote plasma

* Electrochemical Society Student Member.
** Electrochemical Society Active Member.
z E-mail: h.c.m.knoops@tue.nl; w.m.m.kessels@tue.nl

Table I. The material properties of Pt and PtO_2 films deposited at 300°C by thermal and remote plasma ALD from $MeCpPtMe_3$ and O_2 gas or O_2 plasma. In situ SE, XRR, AFM, RBS, and FPP measurements were used for analysis. The typical experimental errors are given in the first row.

Material	ALD process	Thickness (nm) SE	Thickness (nm) XRR	Roughness (nm)	Growth per cycle (Å/cycle)	Mass density (g cm^{-3}) XRR	Mass density (g cm^{-3}) RBS	Atomic composition (atom %) Pt	O	C	Electrical resistivity (μΩ cm)
Pt	5 s O_2 gas[a]	27.3 ± 0.5	26.6 ± 0.3	0.7 ± 0.3	0.45 ± 0.04	22 ± 1	20.8 ± 0.5	100	<5	<5	13 ± 1
Pt	0.5 s remote plasma	~30 [b]	29.2	0.4	0.47	22	20.0	100	<5	<5	15
PtO_2	5 s remote plasma	26.7	26.5	0.4	0.47	10	8.9	31	69	<5	$>1 \times 10^8$

[a] Includes a 7 nm Pt seed layer deposited by the remote plasma ALD process.
[b] Thickness determination less accurate due to opacity of the film at SE wavelengths.

ALD. The remote plasma process of Pt shows a similar growth rate as the thermal process, which in turn is close to that reported by Aaltonen et al. (~0.045 nm/cycle).[1]

The PtO_2 process (5 s O_2 plasma) also shows immediate growth with potentially a brief nucleation delay. After ~50 cycles the growth per cycle is constant at 0.047 nm/cycle compared to ~0.055 nm/cycle found by Hämäläinen et al. using $Pt(acac)_2$ and O_3.[13] From the difference in Pt atomic density, it is concluded that for PtO_2, fewer Pt atoms are deposited per cycle than for the Pt process (1.1×10^{14} Pt cm^{-2} cycle^{-1} for PtO_2 compared to 3.0×10^{14} Pt cm^{-2} cycle^{-1} for Pt). This is different from the thermal Ru and RuO_2 ALD process where the growth rate increases with the partial O_2 pressure going from Ru to RuO_2 material.[16]

The dielectric functions determined by SE for Pt and for PtO_2 are shown in Fig. 2. The two materials result in very distinct dielectric functions, whereas the dielectric functions for Pt obtained by thermal ALD and remote plasma ALD are indistinguishable. The Pt was modeled using a Drude–Lorentz parametrization, where the Drude term, dominant at low photon energies, accounts for the intraband absorption by conduction electrons. Several Lorentz oscillators (at 0.9, 1.5 eV, and higher energies) were used for the interband absorption.[17] In agreement with its semiconductive nature, the dielectric function of PtO_2 could be parametrized by a single Tauc–Lorentz oscillator (0.9 eV bandgap and 4.8 eV peak energy).[18] The optical Tauc bandgap was ~1.5 eV, which is close to the bandgap reported for sputtered amorphous PtO_2 (1.2–1.3 eV).[8]

Material properties.— As shown in Table I both the remote plasma and thermal ALD process result in very similar material properties for the Pt films. In both cases high density (~21 g/cm^3), low resistivity (~15 μΩ cm), and high purity Pt films were deposited. The density and resistivity for these ~30 nm thick films are close to the bulk values of 21.4 g/cm^3 and 10.8 μΩ cm, and they are similar to the values reported for thermal ALD of Pt.[1,3] The O and C contents remain below the RBS detection limit (<5%) and grazing incidence XRD spectra (Fig. 3) revealed a cubic phase composition for both the thermal and remote plasma ALD Pt films. The relatively high intensity of the (220) peak indicates that the Pt crystallites have a preferred orientation with their (111) lattice planes parallel to the sample surface as also reported for the thermal ALD process.[1,2] The remote plasma ALD Pt film, which is only slightly thicker than the thermal ALD film, shows much stronger diffraction peaks, indicating a higher crystallinity. Both processes resulted in smooth films and had generally lower root-mean-square roughness values (0.4–0.7 nm) than reported (0.75–4 nm).[1-3] Because island growth is known to promote surface roughening,[19] the fast nucleation and, consequently, more pronounced layer-by-layer growth can be related to the lower surface roughness obtained for the remote plasma ALD process.

The platinum oxide has a lower density and is slightly overstoichiometric ($PtO_{2.2}$). The resistivity is very high as it is above the detection limit of the FPP (>100 Ω cm). For the process employing $Pt(acac)_2$ and O_3, a lower resistivity (1.5–5 Ω cm) was reported most probably due to a lower O content ($PtO_{1.6}$).[13,20] The

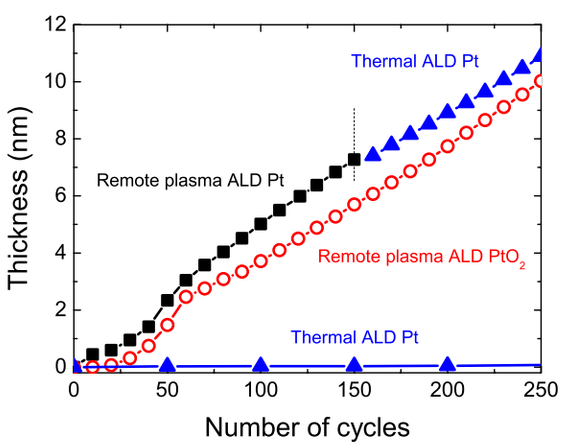

Figure 1. (Color online) Thickness measured by in situ SE as a function of the number of cycles for the Pt and PtO_2 ALD processes. The process conditions are listed in Table I. The starting substrate at 0 cycles was Si(100) with 400 nm SiO_2. After 150 cycles of remote plasma ALD, the Pt film growth is continued by thermal ALD.

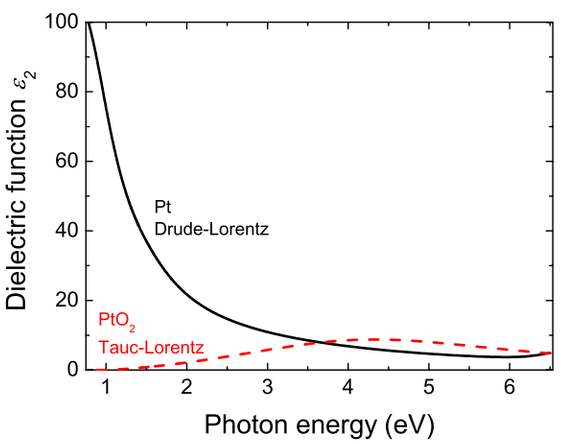

Figure 2. (Color online) The imaginary part of the dielectric function (ε_2) for Pt and PtO_2 as determined by in situ SE measurements evaluated using Drude–Lorentz and Tauc–Lorentz parametrizations, respectively.

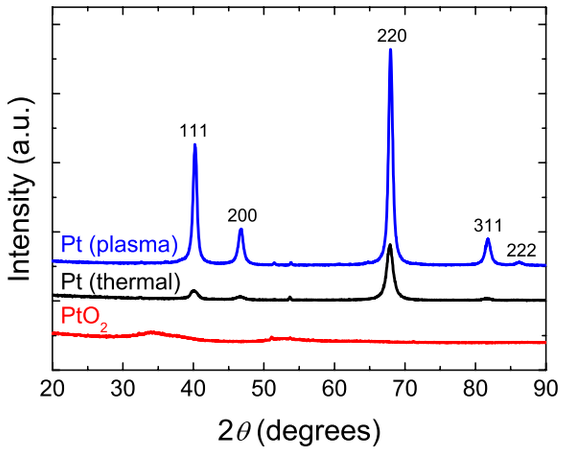

Figure 3. (Color online) Grazing incidence XRD spectra for a remote plasma ALD Pt film (29 nm thickness), a thermal ALD Pt film (27 nm thickness), and a remote plasma ALD PtO_2 film (27 nm thickness). The Miller indexes of cubic Pt are indicated.

PtO_2 film is amorphous or nanocrystalline,[13] and no diffraction peaks from the α and β PtO_2 phases can be identified in the XRD spectra.[8]

Temperature dependence.— Figure 4 shows the growth per cycle for the three processes over a wide temperature range. The thermal ALD Pt process has a temperature window starting at ~200°C. The fact that the growth per cycle is reduced at lower substrate temperatures is not yet understood.[21] From surface science studies, it can be inferred that the dissociative chemisorption of O_2 [on Pt(111)] should not be the limiting factor.[12] On the other hand, the remote plasma ALD process which uses atomic oxygen from the gas phase has a higher growth rate than the thermal process at 200°C. The higher resistivity (~500 μΩ cm) found for this temperature, however, suggests incomplete removal of O and C impurities from the material. The poorer material properties could be overcome by an H_2 plasma treatment. Exposure of the film to 300 s H_2 plasma at 100°C reduced the resistivity to 61 μΩ cm. Moreover, tests with

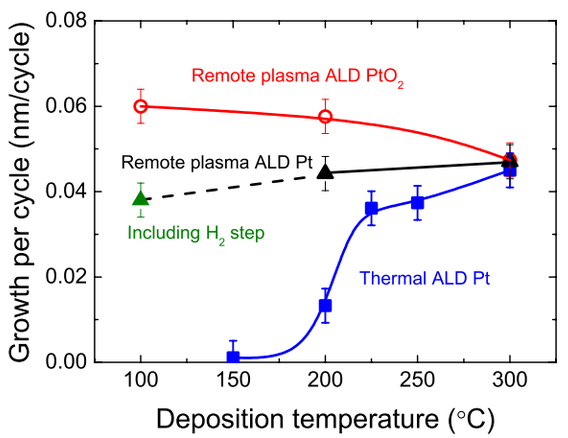

Figure 4. (Color online) The growth per cycle for remote plasma and thermal ALD of Pt and remote plasma ALD of PtO_2 as a function of the substrate temperature. At 100°C the growth rate of the remote plasma process including a H_2 gas exposure step in the ALD cycle is shown. For thermal ALD of Pt, deposition took place on 10 nm thick Pt starting surfaces prepared by remote plasma ALD at 300°C. The lines serve as guides to the eye.

an ALD cycle containing a H_2 gas exposure step (no plasma power applied) of 2 s after the O_2 plasma step resulted in excellent materials properties for Pt at 100°C (mass density of 19.8 g cm^{-3}, no C and O impurities detected, and a resistivity of 19 μΩ cm at 22 nm film thickness). These results demonstrate that the temperature window for remote plasma ALD of Pt can effectively be extended down to 100°C. For PtO_2 the growth per cycle decreases slightly with increasing substrate temperature between 100 and 300°C, demonstrating that this process also has a large temperature window. At the substrate temperature of 300°C, decomposition of PtO_2 is reported to start for sputtered films, while in air decomposition starts at 550°C due to the higher partial pressure of oxygen.[20] For the process employing $Pt(acac)_2$ and O_3, only a small temperature window was observed (120–130°C).[13] Therefore, the large temperature window of our PtO_2 process suggests a higher stability of the material, which can most likely be related to the higher oxygen content ($PtO_{2.2}$ compared to $PtO_{1.6}$).

Conclusions

Remote plasma ALD processes of Pt and PtO_2 were developed from the combination of $MeCpPtMe_3$ precursor and O_2 plasma, and compared to the thermal ALD process of Pt using the same precursor and O_2 gas. High purity Pt can be obtained by a short O_2 plasma exposure, whereas PtO_2 can be obtained by a long O_2 plasma exposure. In situ SE revealed that the remote plasma processes lead to immediate growth without substantial nucleation delay, whereas the thermal ALD process leads to no growth at all unless a Pt starting surface or a high O_2 pressure is employed. A broad temperature window of 100–300°C was achieved for both materials when deposited by remote plasma ALD. For Pt a H_2 gas exposure step was included in the ALD cycle to obtain high purity films at 100°C.

Acknowledgments

This work was sponsored by the Materials Innovation Institute M2i under project no. MC3.06278, and by the Netherlands Technology Foundation STW.

Eindhoven University of Technology assisted in meeting the publication costs of this article.

References

1. T. Aaltonen, M. Ritala, T. Sajavaara, J. Keinonen, and M. Leskelä, *Chem. Mater.*, **15**, 1924 (2003).
2. Y. Zhu, K. A. Dunn, and A. E. Kaloyeros, *J. Mater. Res.*, **22**, 1292 (2007).
3. X. Jiang and S. F. Bent, *J. Electrochem. Soc.*, **154**, D648 (2007).
4. P. H. L. Notten, F. Roozeboom, R. A. H. Niessen, and L. Baggetto, *Adv. Mater. (Weinheim, Ger.)*, **19**, 4564 (2007).
5. M. Armand and J. M. Tarascon, *Nature (London)*, **451**, 652 (2008).
6. L. Baggetto, R. A. H. Niessen, F. Roozeboom, and P. H. L. Notten, *Adv. Funct. Mater.*, **18**, 1057 (2008).
7. R. R. Hoover and Y. V. Tolmachev, *J. Electrochem. Soc.*, **156**, A37 (2009).
8. L. Maya, L. Riester, T. Thundat, and C. S. Yust, *J. Appl. Phys.*, **84**, 6382 (1998).
9. K. Kurihara, Y. Yamakawa, T. Nakano, and J. Tominaga, *J. Opt. A, Pure Appl. Opt.*, **8**, S139 (2006).
10. F. Machalett, K. Gartner, K. Edinger, and M. Diegel, *J. Appl. Phys.*, **93**, 9030 (2003).
11. T. Aaltonen, A. Rahtu, M. Ritala, and M. Leskelä, *Electrochem. Solid-State Lett.*, **6**, C130 (2003).
12. C. T. Campbell, G. Ertl, H. Kuipers, and J. Segner, *Surf. Sci.*, **107**, 220 (1981).
13. J. Hämäläinen, F. Munnik, M. Ritala, and M. Leskelä, *Chem. Mater.*, **20**, 6840 (2008).
14. J. F. Weaver, J. J. Chen, and A. L. Gerrard, *Surf. Sci.*, **592**, 83 (2005).
15. E. Langereis, H. C. M. Knoops, A. J. M. Mackus, F. Roozeboom, M. C. M. van de Sanden, and W. M. M. Kessels, *J. Appl. Phys.*, **102**, 083517 (2007).
16. O. K. Kwon, J. H. Kim, H. S. Park, and S. W. Kang, *J. Electrochem. Soc.*, **151**, G109 (2004).
17. W. S. Choi, S. S. A. Seo, K. W. Kim, T. W. Noh, M. Y. Kim, and S. Shin, *Phys. Rev. B*, **74**, 205117 (2006).
18. G. E. Jellison, Jr. and F. A. Modine, *Appl. Phys. Lett.*, **69**, 371 (1996).
19. R. L. Puurunen and W. Vandervorst, *J. Appl. Phys.*, **96**, 7686 (2004).
20. Y. Abe, M. Kawamura, and K. Sasaki, *Jpn. J. Appl. Phys., Part 1*, **38**, 2092 (1999).
21. T. Aaltonen, M. Ritala, Y. L. Tung, Y. Chi, K. Arstila, K. Meinander, and M. Leskelä, *J. Mater. Res.*, **19**, 3353 (2004).